Performance characteristics of silver cerium vanadate batteries

Abdul Arof, Burhanuddin Kamaluddin, S. Radhakrishna

Classification
Physics Abstracts
86.30D

Performance characteristics of silver cerium vanadate batteries

Abdul Kariem Arof ([1]), Burhanuddin Kamaluddin ([2]) and S. Radhakrishna ([3])

([1]) Physics Division, Centre for Foundation Studies in Science, University of Malaya, 59100 Kuala Lumpur, Malaysia
([2]) Physics Department, University of Malaya, 59100 Kuala Lumpur, Malaysia
([3]) Institute for Advanced Studies, University of Malaya, 59100 Kuala Lumpur, Malaysia

(*Received 1 June 1992, revised 16 February 1993, accepted 10 March 1993*)

Abstract. — Stoichiometric ratios of AR grade AgI, Ag_2O, V_2O_5 and CeO_2 were melted in a furnace and the melt was rapidly quenched to liquid nitrogen temperature to form a glass. The glassy nature of the sample has been confirmed by powder X-ray diffraction technique. The microstructure and microanalysis studies of the silver cerium vanadate (SCV) have been carried out by scanning electron microscopy (SEM) and energy dispersive analysis of X-rays (EDAX). The SEM micrograph of the as-quenched melt showed crystalline AgI precipitate on the surface of the solid as well as glass-in-glass phase separations. The X-ray diffractogram of the powdered SCV sample confirmed the crystalline structure to be AgI. Several batteries were fabricated from the sample, each battery with a 1 : 1 ratio of silver powder and glass in the anode and a 5 : 5 : 1 glass, iodine and carbon mixture in the cathode. The batteries were discharged at 30 μA, 40 μA and 50 μA load currents.

1. Introduction.

Glassy electrolyte materials are normally used in solid state battery systems due to the higher ionic conductivity exhibited over their polycrystalline counterparts and due to their relatively high mechanical strength and low internal resistance. The glassy electrolytes are usually formed by melting the chemical constituents and rapidly quenching them to liquid nitrogen temperature. Many silver based electrolytes using vanadium pentoxide have been prepared in this way [1-5]. Among them are AgI-Ag_2O-V_2O_5 [1, 2], AgI-Ag_2O-B_2O_3-V_2O_5 [3], AgI-Ag_2O-MoO_3-V_2O_5 [4] and AgI-Ag_2O-P_2O_5-V_2O_5 [5]. In this paper, we report the use of a lanthanide oxide, CeO_2 in 70 AgI-20 Ag_2O-3 CeO_2-7 V_2O_5 solid electrolyte as a second glass former. The solid electrolyte is used to fabricate several solid state batteries. Some characteristics of the solid electrolyte and battery are presented and discussed.

2. Experimental.

2.1 MATERIAL PREPARATION. — Stoichiometric ratios (mole %) of AgI, Ag_2O, V_2O_5 and CeO_2 were mixed in different silica crucibles to form 70 AgI-20 Ag_2O-

$10[x\ CeO_2 + (1 - x)\ V_2O_5]$, where $x = 0.2$, 0.3, 0.4, 0.5 and 0.6. The choice of dopant salt concentration is due to the results of an earlier study on the ternary AgI-Ag_2O-V_2O_5 system where the compound 70 AgI-20 Ag_2O-10 V_2O_5 exhibits the highest electrical conductivity of 1.1×10^{-4} S cm^{-1} at room temperature for a glass with a GM : GF ratio of 2 : 1. CeO_2 was added to the ternary system with the hope to further increase the electrical conductivity of the system. The AR grade compounds were melted in a furnace at 1 000 °C and the melts were then poured into a stainless steel container kept in a liquid nitrogen bath to form the glass.

2.2 Material characterization.

2.2.1 *XRD.* — The solid phases obtained were powdered and prepared for X-ray analysis to verify their glassy nature. A Shimadzu XD5 diffractometer was used for this analysis. The wavelength of the X-radiation was 1.542 Å and the X-ray tube was operated at 20 kV and 40 mA.

2.2.2 *Electrical conductivity.* — The electrical conductivity of each sample was measured at room temperature, 300 K using a Philips PM6306 LCR meter operating at 1 kHz. The powdered samples were pelletised and both circular faces (diameter 1.0 cm) of the pellet were coated with silver conductive paint. When the paint dried, the samples were mounted in a conductivity mount with silver leads for attachment to the LCR meter.

2.2.3 *Microstructure and microanalysis.* — Microstructure and microanalysis on the as-quenched sample with composition having the highest electrical conduction was carried out to confirm the crystalline peaks observed in the XRD pattern and to check for glass-in-glass phase separations. The Philips SEM 515 equipment was used to obtain the micrographs and energy dispersive analysis of X-rays (EDAX) was carried out with a Philips 9800 equipment. With the aid of ZAF corrections, quantitative analysis of the chemical composition of the phases in the sample was determined. The SEM micrographs were taken at an accelerating voltage of 20 kV and the EDAX for 100 s.

2.3 Battery fabrication. — The anode of each battery contains silver and electrolyte powders in a 1 : 1 weight ratio. These were well mixed in an argate mortar and 0.25 g of it was poured into a die. Since silver is readily oxidized, the anode serves as an electron reservoir and hence is a negative terminal of the battery. Then 1.05 g of the electrolyte was poured on top of the anode powder layer in the die and the two layers were pressed together under a pressure of 2 tonne to form a two-layered 1.0 cm diameter disc. The cathode contains iodine, electrolyte and carbon in a 5 : 5 : 1 weight ratio and 0.25 g of this mixture was put into a cleaned die to form another 1.0 cm diameter disc. Carbon in the cathode mixture serves as an electron conductor. The cathode receives electron from the external circuit and hence is the positive terminal of the battery. The cathode disc was then placed over the electrolyte surface of the anode-electrolyte disc and clamped between two copper current collectors with leads for external connections.

2.4 Battery characterization.

2.4.1 *Open circuit voltage* (OCV) *and transference number measurements.* — The OCV of the fabricated battery was measured with a 4 1/2 digit multimeter and the transference number was measured following the emf method [6].

2.4.2 *Internal resistance measurements.* — The fabricated battery was connected in series to a decade resistance box (initially set to maximum resistance) and a digital multimeter to measure current through the circuit. A digital multimeter was also connected across the battery to

monitor its voltage. As the resistance was decreased, current begins to flow in the circuit and due to the internal resistance of the battery, the voltage of the battery decreases. Each time the resistance was decreased, the current through the circuit and the voltage were recorded. Several current-voltage readings were obtained. The circuit was then modified to include a commercial battery of higher emf than the fabricated one. The positive terminal of the commercial battery was connected in series with the cathode of the fabricated battery *via* the decade resistance box and the negative terminal of the commercial battery was connected in series with the anode of the fabricated battery *via* a digital ammeter. The resistance of the decade resistance box was once again set to maximum. The battery was allowed to regain its initial OCV. Once this has been achieved, the resistance of the decade resistance box was reduced. The direction of current flow in the circuit is now in the reverse direction to that in the former circuit configuration. The digital ammeter registers a negative current, but the voltmeter registers an increase in the OCV of the fabricated battery. Several current and voltage readings were recorded for the latter circuit configuration. Finally the readings were plotted in a voltage-current graph. The points followed the equation $V = E - Ir$ where V is the voltage of the fabricated battery when current I flows in the circuit, E is the OCV when no current flows from the battery and r is the internal resistance of the battery.

2.4.3 *Discharge characteristics.* — Three other batteries were fabricated from the electrolyte with the highest conductivity and which provides the lowest internal resistance in the battery. These were discharged at load currents of 30 μA, 40 μA and 50 μA.

3. Results and discussion.

3.1 XRD. — Figures 1a-d illustrate the XRD of every chemical component used in the making of the SCV glass. Figure 2 shows the XRD pattern of the various SCV samples with different CeO_2 concentration. The peaks in each diffractogram correspond to AgI peaks [7] except for the sample with 6 mole % CeO_2 which also contain other peaks. Reports on AgI-$AgPO_3$ [8] have also indicated such observations and the structure of AgI was assigned to be that of β or γ. The correlation length of the XRD peak at 2 θ approximately 24° is 5.0, 3.0, 4.4, 3.8 and 4.3 Å for samples containing 2, 3, 4, 5 and 6 mole % CeO_2 respectively. This shows that the phase containing 3 mole % CeO_2 is the most amorphous or glassy in nature.

3.2 ELECTRICAL CONDUCTIVITY. — Figure 3 depicts the electrical conductivity of phases with different CeO_2 content and their impedances. It can be observed that at 300 K, the electrical conductivity of the 70 AgI-20 Ag_2O-3 CeO_2-7 V_2O_5 sample is the highest at 4.0×10^{-4} S cm^{-1}. The impedance for the phases with 2, 3, 4, 5 and 6 mole % CeO_2 is 378 Ω, 103 Ω, 222 Ω, 182 Ω and 200 Ω respectively. The fact that the phase with 3 mole % CeO_2 has the highest electrical conductivity supports the evidence that it is the most amorphous or glassy phase as indicated by comparing the correlation length of the first XRD peak for each sample since glasses are more conducting than polycrystallines. The value of electrolyte impedance for each sample shows the same degree of crystallinity as the correlation length. The conductivity of the quarternary samples are found to be higher than that of the 70 AgI-20 Ag_2O-10 V_2O_5 ternary silver vanadate system. The conductivity-composition plot also seems to indicate the possibility of another peak being present since the conductivity of the SCV sample with $x = 0.6$ is greater than the conductivity of the SCV sample with $x = 0.5$. Observations of more than one peak in the conductivity-composition plot have been reported [9, 10]. This is attributed to the mixed former effect.

3.3 MICROSTRUCTURE AND MICROANALYSIS. — The SEM micrograph, figure 4, of the as-quenched sample with the highest electrical conductivity shows the presence of a crystalline

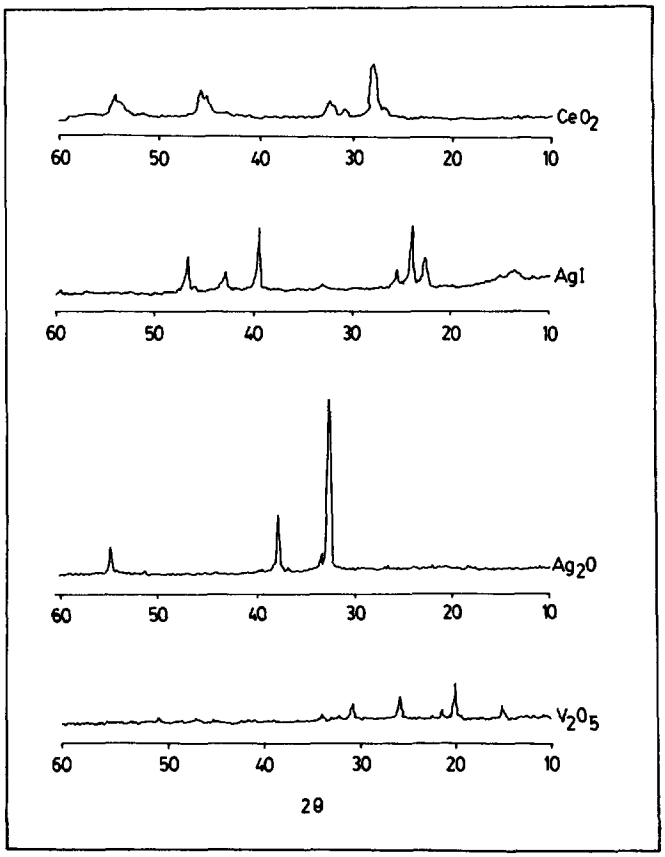

Fig. 1. — X-ray diffractograms of the chemical constituents used in making the SCV samples.

phase and different glass-in-glass phase separations. The crystalline phase explains the observed AgI peaks in the 70 AgI-20 Ag_2O-3 CeO_2-7 V_2O_5 sample. The occurrence of crystalline-in-glass phase separation could be due to the extent of the miscibility gap in the glassy Ag_2O-CeO_2-V_2O_5 network as reported by some authors [11]. Also the presence of crystalline AgI suggests that the AgI in the melt did not interact chemically with the Ag_2O-CeO_2-V_2O_5 network but merely acts as a plasticizing agent as in polymer diluent systems, a fact which is usually concluded from IR spectroscopy studies [12]. The theoretical starting composition for this sample is $Ag_{35.4}I_{22.6}V_{4.5}CeO_{19.8}$ and the starting percentage of each element (excluding oxygen) is 55.9 % (Ag), 35.6 % (I), 7.1 % (V) and 1.5 % (Ce). EDAX analysis, figure 5 reveals that CeO_2 is not present in certain microregions of the sample, while certain microregions detected contains CeO_2 from as low as 0.36 % to as high as 2.01 %. The theoretical composition of Ag, I and V are also within the detected range of 42.54 % to 60.30 %, 27.46 % to 46.16 % and 0.78 % to 13.13 % respectively. An interesting feature from EDAX analysis is the presence of Si which is believed to have been derived from the possible dissolution of silica crucible into the melt. Si is known to induce phase separations in non-silicate glasses [13].

3.4 OCV, TRANSFERENCE NUMBER AND INTERNAL RESISTANCE. — The OCV for all the batteries fabricated is $\approx$ 0.680 V providing a transference number of greater than 0.9 since the

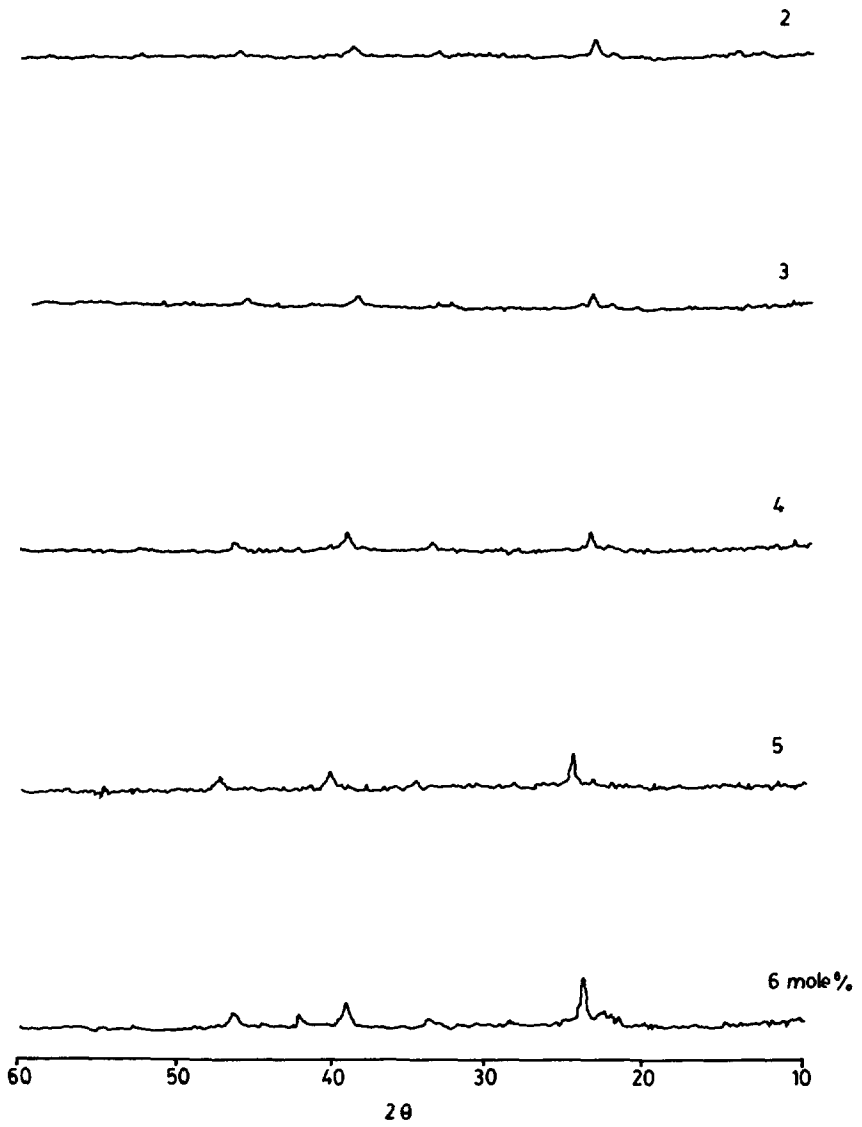

Fig. 2. — XRD pattern of SCV samples containing various concentrations of CeO_2.

theoretical OCV for such silver/iodine battery is 0.687 V [14]. This result indicates that the 70 AgI-20 Ag_2O-3 CeO_2-7 V_2O_5 phase is an ionic conductor and hence is a solid electrolyte. It is clear from figure 6 that the battery fabricated from the SCV sample with composition 70 AgI-20 Ag_2O-7 V_2O_5-3 CeO_2 has the least internal resistance. The electrolyte with this composition also has the highest electrical conductivity. The internal resistance of the SCV batteries with 2, 3, 4, 5 and 6 mole % CeO_2 is 2 400 Ω, 586 Ω, 2 500 Ω, 1 618 Ω and 7 401 Ω respectively. One can see the vast discrepancy between the internal resistance values and the electrolyte impedance for all the various compositions. The internal resistance of the SCV batteries should be almost equal or the same as the electrolyte impedance since the materials used in both anode and cathode are practically good electrical conductors. The discrepancy between these two resistances can be attributed to the cathode-electrolyte interfacial resistance.

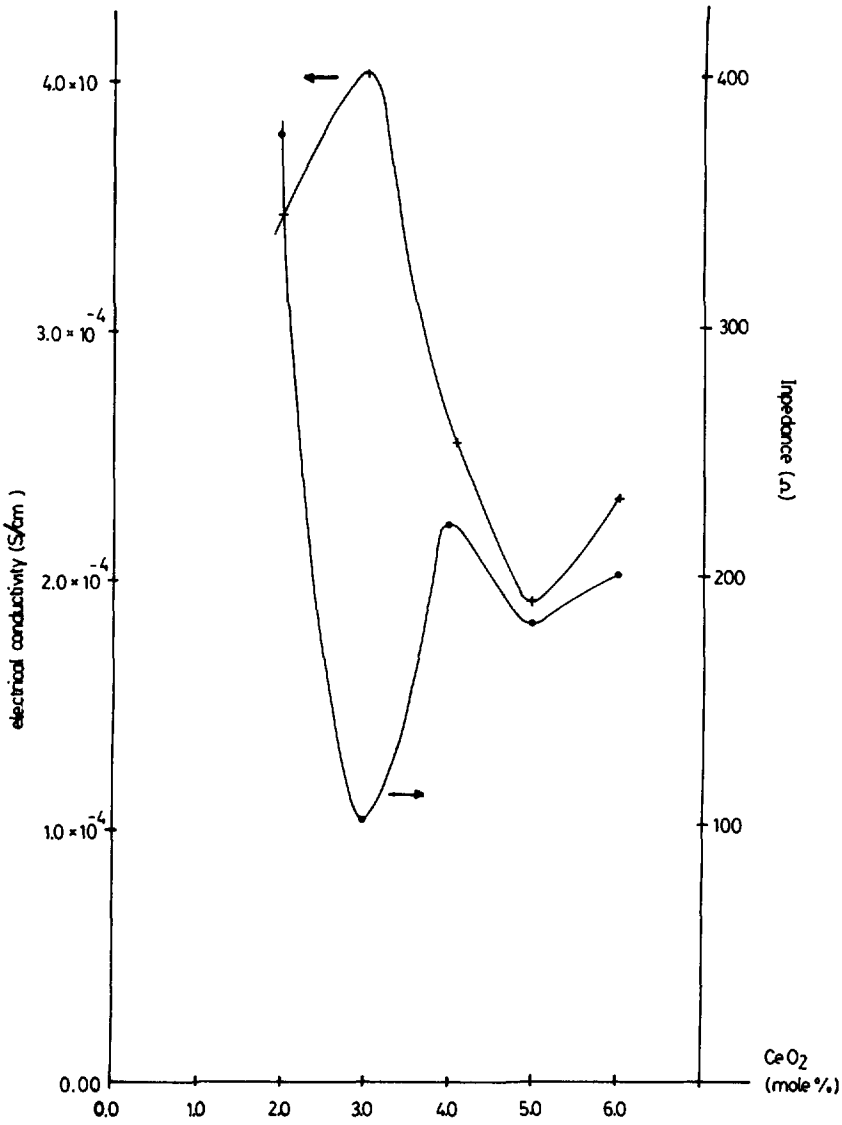

Fig. 3. — Conductivity and impedance of SCV samples pressed at 2 tonne against CeO_2 content.

The electrolyte surface, pressed at 2 tonne is not smooth [15] and hence when the cathode is placed over the electrolyte surface of the anode-electrolyte two layered disc and clamped between two copper current collectors, the contact between the cathode-electrolyte interface can be quite irregular which leads to increased interfacial resistance and internal resistance. To justify this, we have fabricated another battery in which the anode, electrolyte and cathode were all pressed in one solid cylindrical disc under the same compacting pressure as before. The electrolyte impedance is $\approx 160\ \Omega$ and the internal resistance of the battery is 200 Ω. This shows that cathode-electrolyte interfacial resistance contributes to the overall internal resistance of the battery.

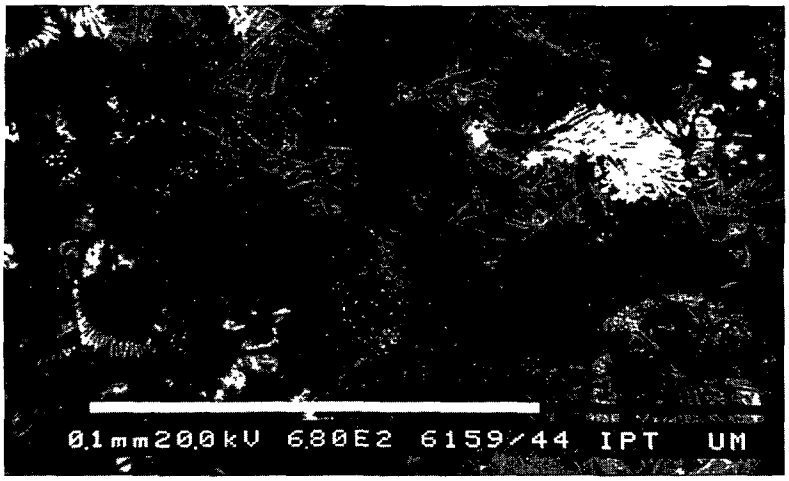

Fig. 4. — Surface morphology of as-quenched 70 AgI-20 Ag_2O-3 CeO_2-7 V_2O_5 SCV sample.

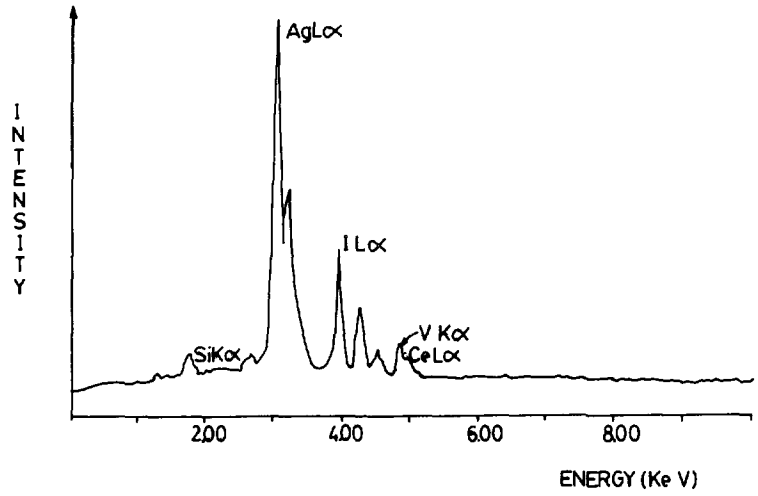

Fig. 5. — EDAX spectrum of 70 AgI-20 Ag_2O-3 CeO_2-7 V_2O_5 as-quenched sample.

3.5 DISCHARGE CHARACTERISTICS. — The discharge characteristics of the SCV batteries at different load currents of 30 μA, 40 μA and 50 μA are as shown in figure 7. It can be observed that the discharge capacity of the battery at 30 μA, 40 μA and 50 μA was 1.56 mAh, 1.00 mAh and 0.50 mAh respectively considering the operating time for the OCV to drop to 540 mV. The energy density was 0.57 Wh/kg, 0.37 Wh/kg and 0.18 Wh/kg at the investigated current loads for a cell weight of 1.55 g. It can also be observed from the discharge curve that on drawing 30 μA from the battery, the voltage dropped to ≈ 600 mV at 0 h. The resistance, R, needed to maintain this current initially was 19.4 kΩ. From $V = I(R + r)$ where V is the voltage of the battery when a current I is drawn out of it, R is the load resistance and r is the internal resistance, the balance of the resistance, r to achieve this voltage is 600 Ω which is approximetely the internal resistance of the battery. The load resistance was reduced

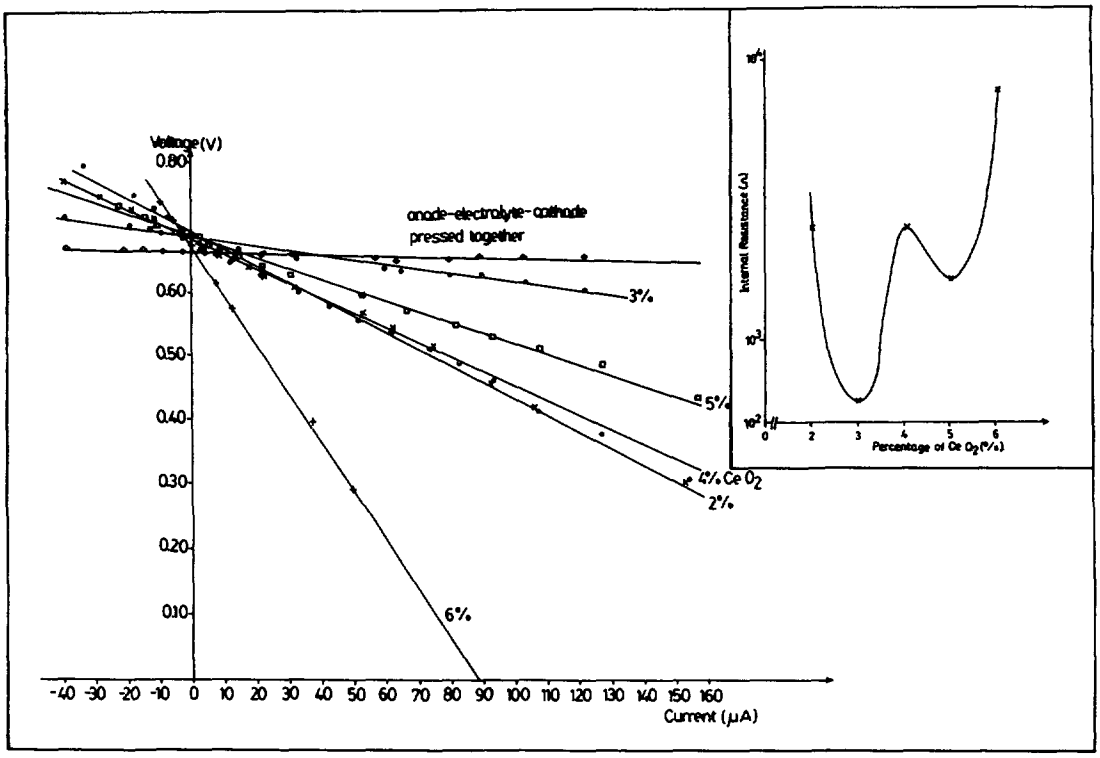

Fig. 6. — Voltage-current characteristics of the SCV batteries. Mole % content of CeO_2 shown. Voltage-current characteristics of battery in which anode-electrolyte-cathode pressed as one single disc is also shown. Inset : Internal resistance of SCV batteries *versus* CeO_2 content (mole %).

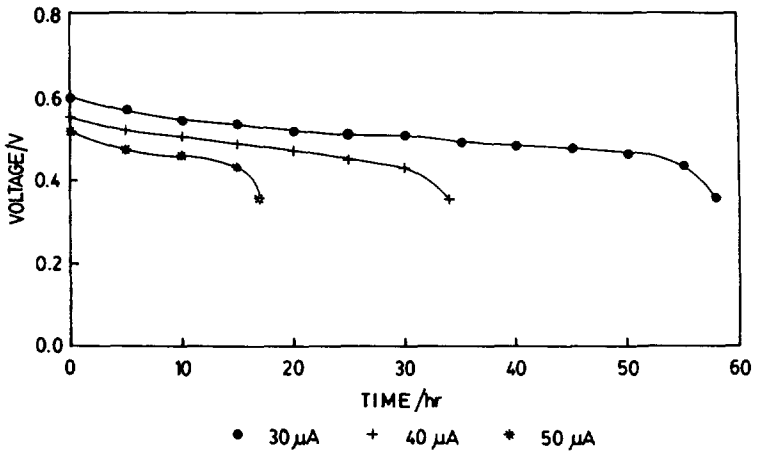

Fig. 7. — Discharge characteristics of SCV batteries.

from time to time in order to maintain the discharge current. The voltage decreased correspondingly when the load resistance was reduced. This was attributable to the formation of the discharge product consisting of the low conducting AgI at ambient temperature within the electrolyte or at the electrode-electrolyte interface which is responsible for the increase in the internal resistance of the battery.

4. Conclusions.

Silver cerium vanadate can be used as an electrolyte for solid state batteries for operating low power consumption devices. The battery performance can be further improved if the electrodes and electrolyte are compacted together as one single disc since there will be no voltage loss due to interfacial resistance between the cathode and electrolyte.

Acknowledgements.

The authors would like to thank Harlina Damiri and Mazni Mohd Nor for technical assistance and the University of Malaya for the votes PJP 155/91 and PJP 71/92. Also to Mr Shaharudin of the Electron Microscopy Laboratory, Institute for Advanced Studies, University of Malaya for the microanalysis and to Mr A. Zakuan for help with the figures.

References

[1] HARIHARAN K., TOMY C. V. and KAUSHIK R., *Bull. Electrochem. 1* **4** (1985) 405-408.
[2] HARIHARAN K., TOMY C. V. and KAUSHIK R., *J. Mat. Sci. Lett.* **4** (1985) 1379-1382.
[3] KAUSHIK R. and HARIHARAN K., *Solid State Ionics* **28-30** (1988) 732-735.
[4] SATYANARAYANA N. and RADHAKRISHNA S., *Solid State Ionics* **28-30** (1988) 811-813.
[5] PRASAD P. S. S. and RADHAKRISHNA S., *J. Solid State Chem.* **76** (1988) 7-17.
[6] CHANDRA S., Superionic Solids : Principles and Applications (North-Holland, Amsterdam, 1981).
[7] Selected Powder Diffraction Data for Minerals, First Edition, Joint Committee on Powder Diffraction Standard (Philadelphia, USA, 1974).
[8] NOWINSKI J. L., WNETRZEWSKI B. and JAKUBOWSKI W., *Solid State Ionics* **28-30** (1988) 804-807.
[9] MAGISTRIS A., CHIODELLI G. and DUCLOT M., *Solid State Ionics* **9/10** (1983) 611.
[10] TOTSUMISAGO M., HAMADA A., MINAMI T. and TANAKA M., *J. Non-Cryst. Solids* **56** (1983) 423.
[11] RINCON J. M., MARQUEZ H. and RIVERA E., *J. Mat. Sci.* **26** (1991) 1192-1198.
[12] LIU J., PORTIER J., TANGUY B., VIDEAU J.-J. and ANGELL C. A., *Solid State Ionics* **34** (1989) 87-92.
[13] Private communication.
[14] LINFORD R. G., *Solid State Ionics* **28-30** (1988) 831-840.
[15] AROF A. K. and RADHAKRISHNA S., *Mat. Sci. Engg.*, to be published.